CHIN. PHYS. LETT. Vol. 33, No. 7 (2016) 070302

Combined Effect of Classical Chaos and Quantum Resonance on Entanglement Dynamics *

Jin-Tao Tan(谭金桃)[1], Yun-Rong Luo(罗云荣)[1], Zheng Zhou(周政)[2], Wen-Hua Hai(海文华)[1]**

[1]*Department of Physics and Key Laboratory of Low-dimensional Quantum Structures and Quantum Control of Ministry of Education, and Synergetic Innovation Center for Quantum Effects and Applications, Hunan Normal University, Changsha 410081*

[2]*Department of Physics and Mathematics, Hunan Institute of Technology, Hengyang 421002*

(Received 18 April 2016 and accepted by Ying Wu)

We use linear entropy of an exact quantum state to study the entanglement between internal electronic states and external motional states for a two-level atom held in an amplitude-modulated and tilted optical lattice. Starting from an unentangled initial state associated with the regular 'island' of classical phase space, it is demonstrated that the quantum resonance leads to entanglement generation, the chaotic parameter region results in the increase of the generation speed, and the symmetries of the initial probability distribution determine the final degree of entanglement. The entangled initial states are associated with the classical 'chaotic sea', which do not affect the final entanglement degree for the same initial symmetry. The results may be useful in engineering quantum dynamics for quantum information processing.

PACS: 03.67.Mn, 05.45.Ac, 03.65.Vf DOI: 10.1088/0256-307X/33/7/070302

In recent years, quantum entanglement (hereafter simply entanglement), central to foundations of quantum theory,[1] has been regarded as a crucial resource which can be exploited to perform many useful tasks in quantum information processing.[2–8] A great deal of theoretical and experimental effort has been given to the entanglement dynamics for two-electron atomic systems[9] and for molecular systems,[10] and to the ultrafast generation of spin-motion entanglement using a short train of picosecond pulses.[11] Much more attention was paid to the connection between entanglement and chaos,[12,13] due to the challenges in identifying quantum signature in classically chaotic systems.[14–16] For a multipartite quantum kicked top model, studies on the bipartite and the pairwise entanglement whose dynamics depend on initial state in different regions of the phase space and the time-averaged entangling power depending on the strength of the chaoticity parameter in the Hamiltonian revealed that entanglement is a strong signature of the classical chaos.[17] Subsequently, in a similar system, Chaudhury *et al.* provided experimental evidence for dynamical entanglement as a quantum signature of chaos.[15] For an N-atom Jaynes–Cummings model, it was found that for a short time, a faster increase in entanglement, quantitatively expressed in terms of the reduced density linear entropy, can be shown for the chaotic initial conditions as compared with the regular ones.[18] The chaos-assisted quantum dynamical tunneling between separated momentum regions in classical phase space has been observed in an amplitude-modulated optical lattice system.[19,20] Adding a static tilt to the amplitude-modulated system, the localization of off-resonance case and the resonance-assisted quantum tunneling were shown, where the quantum resonance means the modulation frequency to fit the static tilt.[21] Some near-resonant regions, cross chaotic and regular regions in the parameter space were found, in which chaos-assisted quantum tunneling was displayed.[22] Therefore, it is interesting to study the combined effect of classical chaos and quantum resonance on the entanglement dynamics in the amplitude-modulated and tilted optical lattice.

In this Letter, we consider a single two-level atom with two stable internal (electronic) ground states,[23] which is held in a one-dimensional amplitude-modulated and tilted optical lattice. We will exactly analyze the entanglement dynamics between the internal electronic state and the external motional state, and quantify it using the linear entropy related to the purity of the reduced density matrix. Applying the resonance parameter and unentangled initial states, we theoretically illustrate that the linear entropy increases more rapidly for parameters in the chaotic region than that in the regular region. The initial entangled states are associated with the 'chaotic sea' of classical phase space and their time evolutions are adjusted by the phases of the initial states. The final degree of entanglement only depends on the symmetries of the initial probability distributions in both the entangled and untangled initial states cases.

We consider a single two-level atom with two stable internal (electronic) ground states $|g_\alpha\rangle$ obeying $\langle g_\beta|g_\gamma\rangle = \delta_{\beta\gamma}$ for $\alpha,\beta = 1,2$ held in a one-dimensional (1D) amplitude-modulated and tilted op-

*Supported by the National Natural Science Foundation of China under Grant Nos 11175064 and 11475060, the Construct Program of the National Key Discipline of China, and the Hunan Provincial Innovation Foundation for Postgraduates under Grant No CX2014B195.

**Corresponding author. Email: whhai2005@aliyun.com

© 2016 Chinese Physical Society and IOP Publishing Ltd

tical lattice potential,[19,20,22] which can be realized experimentally.[23,24] In the nearest-neighbor tight binding approximation, quantum dynamics of the system is governed by the Hamiltonian[22–26]

$$H_\alpha(t) = \sum_{\alpha=1}^{2}\sum_{m=-\infty}^{\infty}[J_\alpha(t)(|m\rangle|g_\alpha\rangle\langle g_\alpha|\langle m+1| + \text{H.c.}) - \pi\xi m|m\rangle|g_\alpha\rangle\langle g_\alpha|\langle m|], \quad (1)$$

where H has been normalized in units of the recoil energy $E_\text{r} = \frac{\hbar^2k^2}{2m}$, and $|m\rangle$ represents the Wannier state localized on lattice site m. For any fixed α, Eq. (1) describes a single-level atom confined in the amplitude-modulated and tilted lattice potential $V_\alpha(x,t) = [1-\epsilon_\alpha\sin(\omega t)]V_0\sin^2 x + \xi x$ such that the coupling parameter between two adjacent sites is given as[22] $J_\alpha(t) = \int_{-\infty}^{\infty}dx w(x-x_j)[-\nabla^2 + (1-\epsilon_\alpha\sin(\omega t))V_0\sin^2 x]w(x-x_{j+1}) = J_{0\alpha} + \delta J_\alpha\sin\omega t$ by using the Wannier functions $\langle x|j\rangle = w(x-x_j)$ with x_j being the jth lattice site for any integer j. Here the constants $J_{0\alpha}$ and δJ_α are proportional to the depth V_0 and modulated amplitude $-\epsilon_\alpha V_0$ of the optical lattice, which is adjusted by the Rabi frequency.[23] The parameters $J_\alpha(t)$, ω, x and t are normalized in units of E_r, ω_r, k^{-1} and ω_r^{-1} respectively, with the wave vector k, mass m and recoil frequency $\omega_\text{r} = E_\text{r}/\hbar$. The constant $\xi\pi$ (with π being the dimensionless lattice length in the x-coordinate) is the tilt strength in units of kE_r, and the dimensionless constant ϵ_α is the driving amplitude factor. Such a system can be realized experimentally by applying an amplitude-modulated laser standing wave and a linear potential produced by a magnetic field gradient.[21,24] Throughout, we consider a ^{87}Rb atom in a lattice with wavelength $\lambda = 800\,\text{nm}$ and depth $V_0 = 3$ such that the recoil frequency and the time-dependent coupling are computed as $\omega_\text{r} = 22.5\,\text{kHz}$ and $J_\alpha(t) = -0.058 - 0.033\epsilon_\alpha\sin(\omega t)$.

We express the quantum state $|\psi(t)\rangle$ as a superposition of the states $|m\rangle|g_\alpha\rangle$

$$|\psi(t)\rangle = \sum_m[C_{m1}(t)|m\rangle|g_1\rangle + C_{m2}(t)|m\rangle|g_2\rangle], \quad (2)$$

where the complex coefficients $C_{m1}(t)$ and $C_{m2}(t)$ obey a normalization condition

$$\sum_m[(C_{m1}^2(t) + C_{m2}^2(t)] = 1. \quad (3)$$

By substituting Eqs. (1) and (2) into the time-dependent Schrödinger equation $i\frac{\partial|\psi(t)\rangle}{\partial t} = H(t)|\psi(t)\rangle$, we obtain a set of time-evolution equations

$$i\dot{C}_{m\alpha}(t) = J_\alpha(t)(C_{m+1\alpha} + C_{m-1\alpha}) - \pi\xi m C_{m\alpha}, \quad (4)$$

of the probability amplitudes $C_{m\alpha}(t)$ for $\alpha = 1, 2$. We have investigated the same system,[22] and obtained the new analytical solution of the probability amplitude[27]

$$\begin{aligned} C_{m\alpha}(t) &= e^{im\pi\xi t}\sum_{r,n}C_{r\alpha}(0)(-i)^n \\ &\quad\cdot\mathcal{J}_n[2u(t)]\mathcal{J}_{r-m-n}[2v(t)], \\ u(t) &= \int_0^t J_\alpha(\tau)\cos(\pi\xi\tau)d\tau, \\ v(t) &= \int_0^t J_\alpha(\tau)\sin(\pi\xi\tau)d\tau, \end{aligned} \quad (5)$$

where $C_{r\alpha}(0)$ denotes the initial possibility amplitude at site r for the internal state $|g_\alpha\rangle$, $\mathcal{J}_n$ is the nth Bessel functions of the first kind. Such an exact solution is similar to the previous result in Ref. [25], and can be directly proved by inserting Eq. (5) into Eq. (4) and noticing the formulas $\sum_{n=-\infty}^{\infty}(-i)^{n\pm1}\mathcal{J}_{n\pm1}\mathcal{J}_{m-(n\pm1)} = \sum_{n=-\infty}^{\infty}(-i)^n\mathcal{J}_n\mathcal{J}_{m-n}$. In Eq. (5), the resonance condition means the modulation frequency ω in $J_\alpha(t)$ fitting the static tilt[21,22] $|\pi\xi|$.

In the following, we quantify entanglement by computing the linear entropy associated with the reduced density matrix.[28,29] We may also choose the von Neumann entropy[30] as our entanglement measure, and prove that the qualitative results are independent of choice of entropies for the considered pure states. Furthermore, the linear entropy and the von Neumann entropy are two limiting cases of the Rényi entropy.[31]

To estimate the entanglement of $|\psi(t)\rangle$, we have to analyze one of the reduced density operators $\rho_\text{int} = \text{Tr}_\text{mot}(\rho)$ and $\rho_\text{mot} = \text{Tr}_\text{int}(\rho)$. The operator ρ_int of internal state can be calculated by taking the partial trace with respect to the motion state

$$\begin{aligned} \rho_\text{int}(t) &= \text{Tr}_\text{mot}[|\psi(t)\rangle\langle\psi(t)|] \\ &= \sum_m\langle m|\psi(t)\rangle\langle\psi(t)|m\rangle, \end{aligned} \quad (6)$$

and the reduced density matrix (ρ_int) can be expressed in the internal state basis $|g_1\rangle, |g_2\rangle$ as[10]

$$(\rho_\text{int}) = \begin{pmatrix} \sum_m|C_{m1}|^2 & \sum_m C_{m1}C_{m2}^* \\ \sum_m C_{m1}^*C_{m2} & \sum_m|C_{m2}|^2 \end{pmatrix}, \quad (7)$$

with $\text{Tr}(\rho_\text{int}) = 1$. According to Eq. (7), we have the purity of the reduced density matrix

$$\begin{aligned} \text{Tr}[(\rho_\text{int})^2] &= \Big(\sum_m|C_{m1}|^2\Big)^2 + \Big(\sum_m|C_{m2}|^2\Big)^2 \\ &\quad + 2|\sum_m C_{m1}C_{m2}^*|^2. \end{aligned} \quad (8)$$

The linear entropy measuring entanglement can be expressed as[10]

$$L(t) = 1 - \text{Tr}[(\rho_\text{int})^2(t)]. \quad (9)$$

The purity defined by Eq. (8) is bounded and satisfies $1/2 \le \text{Tr}[(\rho_\text{int})^2(t)] \le 1$, and the corresponding linear entropy obeys $0 \le L(t) \le 1/2$. If $\text{Tr}[(\rho_\text{int})^2(t)] = 1$ $(L(t) = 0)$, the internal subsystem is pure by itself.

For a pure state, L vanishes, whereas for a maximally mixed qubit we have $L = 1/2$ in our system.

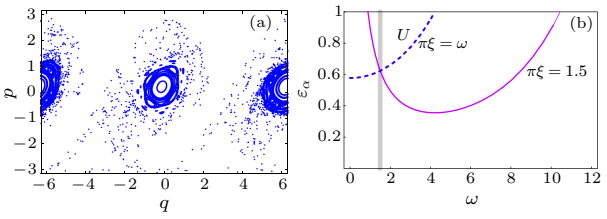

Fig. 1. (Color online) (a) Poincaré section for the rescaled position q and momentum p of a classical particle for the resonant and chaotic parameters $\pi\xi = \omega = 1.5$ and $\epsilon_\alpha = 0.63$. (b) Chaotic and regular parameter regions with different boundary curves for $\pi\xi = 1.5$ (solid curve) and $\pi\xi = \omega$ (thick dashed curve). The resonant line (thick solid curve) is labeled by f. The chaos-resonance overlapping region $f \cap U$ exists above the thick dashed curve. Hereafter all the quantities appearing in the figures are dimensionless. Here $V_0 = 3$.

Fixing the lattice depth $V_0 = 3$, the classically chaotic feature of the considered system with potential $V_\alpha(x,t)$ is shown in Fig. 1. In Fig. 1(a), the Poincaré section is made up of a mixture of regular and chaotic areas of significant size for $\epsilon_\alpha = 0.63$ and the resonance parameters $\pi\xi = \omega = 1.5$, where some small-amplitude 'islands' of stability appearing in the central regions of different potential wells are separated by the 'chaotic sea'.[20,22] The regular 'islands' will disappear gradually with increasing the driving amplitude ϵ_α in chaotic region of parameter space, and global chaos will appear with a critical driving amplitude. For the tilt $\pi\xi = 1.5$, we plot the boundary between chaotic and regular regions in Fig. 1(b) whose upside is the chaotic region of parameter space. A special curve is displayed by the thick dashed curve, which corresponds to the resonant parameters $\pi\xi = \omega$.[21] Therefore, in the region above the curve labeled by U, chaos and resonance may coexist. The resonant line crossing the chaotic and regular regions is labeled by f. The quantum dynamics of the considered system has been shown in the previous work under the initial condition that the particle is placed at the center of the site, namely in the small amplitude 'islands' of stability.[22] Here we are interested in the influence of chaos on entanglement, including driving amplitude ϵ_α in the chaotic region and the different initial conditions corresponding to the classically chaotic sea.

We now explore the dynamics of entanglement for the initial state

$$|\psi(0)\rangle = [C_{01}(0)|g_1\rangle + C_{02}(0)|g_2\rangle]|0\rangle, \qquad (10)$$

with the motional state $|0\rangle$ corresponding to the central regular 'island' in Fig. 1(a), where $|C_{01}(0)|^2 + |C_{02}(0)|^2 = 1$. Clearly, such an initial state is unentangled between the internal and external states, and the corresponding linear entropy vanishes. By applying the resonance parameter, we have discussed the quantum dynamic behavior of the particle,[22] and revealed that the particle will diffuse to both ends of the lattice only for the resonance parameters.[22]

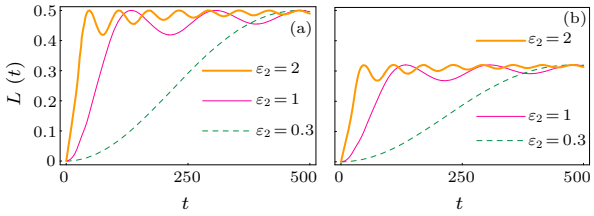

Fig. 2. (Color online) Dynamical evolution of linear entropy $L(t)$ for the parameters $\pi\xi = \omega = 1.5$, $\epsilon_1 = 0.45$, and $\epsilon_2 = 0.3$ (dashed line), $\epsilon_2 = 1$ (solid line), $\epsilon_2 = 2$ (thick solid line), and the initial condition (a) $C_{01}(0) = C_{02}(0) = 1/\sqrt{2}$, (b) $C_{01}(0) = 1/\sqrt{5}$ and $C_{02}(0) = 2/\sqrt{5}$.

Applying the exact solution in Eqs. (2) and (5) to the linear entropy in Eq. (9), one can investigate entanglement dynamics of the system. For convenience, we fix the resonance parameters $\pi\xi = \omega = 1.5$ and the driving strength $\epsilon_1 = 0.45$ in the regular region of Fig. 1(b) and vary ϵ_2 from regular ($\epsilon_2 = 0.3$) to chaotic ($\epsilon_2 = 1, 2$) regions. In the calculations, the exact solution has been truncated with m from -100 to 100 and n from -20 to 20. Time evolutions of the linear entropy $L(t)$ are displayed in Fig. 2 for Fig. 2(a) the initially symmetric probability distribution $C_{01}(0) = C_{02}(0) = 1/\sqrt{2}$ and Fig. 2(b) the initially asymmetric probability distribution $C_{01}(0) = 1/\sqrt{5}$ and $C_{02}(0) = 2/\sqrt{5}$. In both cases, we observe that the linear entropy increases from the initial zero to the maximal values with different speeds, and finally tends to the different maximal values. The parameters in the chaotic region correspond to greater generation speed of entanglement than that in the regular region, and the generation speed is positively related to the driving strength in both regions. Particularly, for any driving strength the initially symmetric and asymmetric probability distributions lead to the final maximal values of linear entropy 0.5 and 0.33, respectively. This means that the symmetries of the initial probability distribution determine the final degree of entanglement.

In the nearest-neighbor tight binding approximation, quantum correspondence of the classically chaotic sea means that the occupying site of the particle should deviate from the central position of a single potential well. The corresponding initial conditions should be related to some superposition states, for example,

$$|\psi(0)\rangle = \sqrt{0.5}(C_{01}|0\rangle + C_{11}|1\rangle)|g_1\rangle + \sqrt{0.5}(C_{02}|0\rangle + C_{12}e^{i\theta}|1\rangle)|g_2\rangle, \qquad (11)$$

with constant phase θ. Here we consider the simplest case where the initial probability amplitudes in the sites 0 and 1 are the same, $C_{01} = C_{11} = C_1$ and $C_{02} = C_{12} = C_2$. Thus the initial state in Eq. (11) is an entangled one for the phase $\theta \neq 2n'\pi$, $n' = 0, 1, \ldots$ that means the entangled initial states associated with the classical chaotic sea. The initial conditions we

consider can be experimentally realized by means of loading atoms around a barrier of the used potential $V_0 \sin^2 x$ one by one from a deterministic source of single atoms.[32] We plot time evolutions of linear entropy $L(t)$ in Fig. 3 for $\epsilon_2 = 1$ and the same other parameters as those of Fig. 2, and the phases $\theta = 0, \frac{\pi}{3}, \frac{\pi}{2}, \frac{2\pi}{3}, \pi$, respectively. Figure 3(a) is associated with the initially symmetric probability distribution $C_1(0) = C_2(0) = 1/\sqrt{2}$, and Fig. 3(b) corresponds to the initially asymmetric probability distribution $C_1(0) = 1/\sqrt{5}$ and $C_2(0) = 2/\sqrt{5}$. The linear entropy generally oscillates with time for any initial condition and any phase, and finally tends to the same maximal value as that of Fig. 2. This means that the entangled initial states do not affect the final entanglement degree for the same symmetry.

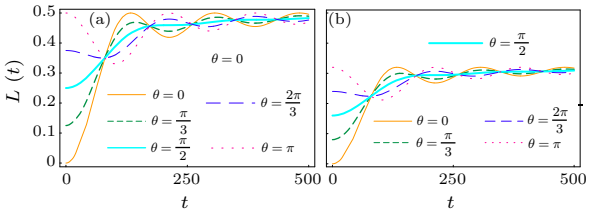

Fig. 3. (Color online) Time evolutions of linear entropy $L(t)$ for $\pi\xi = \omega = 1.5$, $\epsilon_1 = 0.45$, $\epsilon_2 = 1$, and $\theta = 0$ (solid curve), $\theta = \frac{\pi}{3}$ (thick dashed curve), $\theta = \frac{\pi}{2}$ (thick solid curve), $\theta = \frac{2\pi}{3}$ (long dashed curve) and $\theta = \pi$ (dotted curve). The initial conditions (a) $C_1(0) = C_2(0) = 1/\sqrt{2}$ and (b) $C_1(0) = 1/\sqrt{5}$ and $C_2(0) = 2/\sqrt{5}$ are adopted.

In addition, we have also considered the off-resonance case with the modulation frequency not fitting the static tilt. It is found that for any parameter set with nonzero tilt, the particle is generally localized around the initial place such that an unentangled initial state will result in an approximate zero linear entropy, and an entangled initial state corresponds to a constant linear entropy in time evolution.

In summary, using an exact quantum state, we have investigated the entanglement (quantified by linear entropy) dynamics of a single atom held in a one-dimensional amplitude-modulated and tilted optical lattice. Under the quantum resonance conditions and for the regular and chaotic regions in parameter space, it is theoretically demonstrated that for an unentangled initial state, the generation speed of entanglement is faster for the chaotic parameter than for the regular one, and the symmetries of the initial probability distribution determine the final degree of entanglement. The relation between the entangled initial states and the classical chaotic sea is revealed, which does not affect the final entanglement degree for the same initial symmetry. Those results can be applied to engineer quantum dynamics for quantum information processing.

References

[1] Horodecki R, Horodecki P, Horodecki M and Horodecki K 2009 *Rev. Mod. Phys.* **81** 865
[2] Loyd S 1993 *Science* **261** 1569
[3] Bennett C H and Wiesner S J 1992 *Phys. Rev. Lett.* **69** 2881
Bennett C H, Brassard G, Crépeau C, Jozsa R, Peres A and Wootters W K 1993 *Phys. Rev. Lett.* **70** 1895
[4] Cleve R, Gottesman D and Lo H K 1999 *Phys. Rev. Lett.* **83** 648
[5] Nielsen M A and Chuang I L 2000 *Quantum Computation and Quantum Communication* (Cambridge: Cambridge University Press)
[6] Tang S Q, Yuan J B, Wang X W and Kuang L M 2015 *Chin. Phys. Lett.* **32** 040303
[7] Song W, Huang Y S, Yang M and Cao Z L 2015 *Chin. Phys. Lett.* **32** 088701
[8] Zhu W T, Ren Q B, Duan L W and Chen Q H 2016 *Chin. Phys. Lett.* **33** 050302
[9] Osenda O and Serra P 2007 *Phys. Rev.* A **75** 042331
Lin Y C, Lin C Y and Ho Y K 2013 *Phys. Rev.* A **87** 022316
[10] Vatasescu M 2013 *Phys. Rev.* A **88** 063415
[11] Mizrahi J, Senko C, Neyenhuis B, Johnson K G, Campbell W C, Conover C W S and Monroe C 2013 *Phys. Rev. Lett.* **110** 203001
[12] Lü X Y, Jing H, Ma J Y and Wu Y 2015 *Phys. Rev. Lett.* **114** 253601
[13] Fratini E and Pilati S 2015 *Phys. Rev.* A **91** 061601(R)
[14] Haake F 1991 *Quantum Signature of Chaos* (Berlin: Springer)
[15] Chaudhury S, Smith A, Anderson B E, Ghose S and Jessen P S 2009 *Nature* **461** 768
[16] Emerson J, Weinstein Y S, Lloyd S and Cory D G 2002 *Phys. Rev. Lett.* **89** 284102
Xie Q T and Hai W H 2005 *Eur. Phys. J.* D **33** 265
[17] Wang X G, Ghose S, Sanders B C and Hu B 2004 *Phys. Rev.* E **70** 016217
[18] Furuya K, Nemes M C and Pellegrino G Q 1998 *Phys. Rev. Lett.* **80** 5524
[19] Steck D A, Oskay W H and Raizen M G 2001 *Science* **293** 274
Steck D A 2009 *Nature* **461** 736
[20] Hensinger W K, Haffner H, Browaeys A, Heckenberg N R, Helmerson K, McKenzie C, Milburn G J, Phillips W D, Rolston S L, Rubinsztein-Dunlop H and Upcroft B 2001 *Nature* **412** 52
[21] Ma R, Tai M E, Preiss P M, Bakr W S, Simon J and Greiner M 2011 *Phys. Rev. Lett.* **107** 095301
[22] Tan J T, Lu G B, Luo Y L and Hai W H 2014 *Chaos* **24** 043114
[23] Gardiner S A, Cirac J I and Zoller P 1997 *Phys. Rev. Lett.* **79** 4790
[24] Chen Y A, Nascimbene S, Aidelsburger M, Atala M, Trotzky S and Bloch I 2011 *Phys. Rev. Lett.* **107** 210405
[25] Dunlap D H and Kenkre V M 1986 *Phys. Rev.* B **34** 3625
[26] Chen H, Tan J T, Hai K, Zhang X L and Hai W H 2015 *Eur. Phys. J.* D **69** 278
[27] Tan J T, Zou M L, Luo Y L and Hai W H 2016 *Chaos* **26** 063106
[28] Sun Y H, Zhu X and Kuang L M 2005 *Chin. Phys. Lett.* **22** 1833
[29] Liao Q H, Fang G Y, Wang Y Y, Ahmad M A and Liu S T 2010 *Chin. Phys. Lett.* **27** 070304
[30] Vedral V 2002 *Rev. Mod. Phys.* **74** 197
Vedral V and Plenio M B 1998 *Phys. Rev.* A **57** 1619
[31] Rényi A 1970 *Probability Theory* (Amsterdam: North-Holland)
[32] Kuhr S, Alt W, Schrader D, Müller M, Gomer V and Meschede D 2001 *Science* **293** 278